Cleveland State University
EngagedScholarship@CSU

Mechanical Engineering Faculty Publications

Mechanical Engineering Department

5-2011

Characterization of Fracture Toughness G (sub c) of PVC and PES Foams

Elio E. Saenz
Florida Atlantic University, esaenz@fau.edu

Leif A. Carlsson
Florida Atlantic University, Carlsson@fau.edu

Anette M. Karlsson
Cleveland State University, a.karlsson@csuohio.edu

Follow this and additional works at: https://engagedscholarship.csuohio.edu/enme_facpub

Part of the Mechanical Engineering Commons

How does access to this work benefit you? Let us know!

Original Citation

Saenz, E. E., Carlsson, L. A., and Karlsson, A., 2011, "Characterization of Fracture Toughness G (sub c) of PVC and PES Foams," Journal of Materials Science, 46(9) pp. 3207-3215.

Characterization of fracture toughness (G_c) of PVC and PES foams

Elio E. Saenz · Leif A. Carlsson · Anette Karlsson

Abstract The fracture behavior of polyvinyl chloride (PVC) and polyethersulfone (PES) foams has been examined using the single-edge notch bend and the double cantilever beam (DCB) tests. PVC foam densities ranging from 45 to 100 kg/m^3 and PES foam densities ranging from 60 to 130 kg/m^3 were examined. The PVC foams failed in a linear elastic brittle manner, whereas the PES foams displayed much more ductility and substantially larger toughness at a comparable foam density. The cell wall thickness of the PES foams was almost twice the thickness of the PVC foams which may have contributed to the high fracture toughness here defined as critical energy release rate (G_c). The PES foam, further displayed low initiation toughness, due to the sharp artificial crack tip and large toughness corresponding to propagation from a natural crack. The results show that the ductile PES foams have toughness close to its solid counterpart whereas the toughness of the PVC foams falls substantially below its solid counterpart.

E. E. Saenz (✉) · L. A. Carlsson
Department of Ocean and Mechanical Engineering,
Florida Atlantic University, Boca Raton, FL 33431, USA
e-mail: ESaenz@fau.edu

L. A. Carlsson
e-mail: Carlsson@fau.edu

A. Karlsson
Department of Mechanical Engineering,
University of Delaware, Newark, DE 19716, USA
e-mail: Karlsson@udel.edu

Introduction

Sandwich structures may fail in a range of failure modes governed by the specific loading configuration and mechanical properties of the face sheets and core. Such failure modes dictate how a sandwich structure should be designed and constructed [1]. Foam cores are very popular in several structural sandwich applications. The "effective density", ρ^*, which is the apparent density of the foam divided by the density of the solid, of polymer foams typically lies between 0.03 and 0.15, which shows that the majority of the foam volume is occupied by air. Hence foams are generally weak and frequently govern the failure of a sandwich structure.

This paper considers microstructural characterization and evaluation of the fracture behavior of two commercial foams, viz. polyvinyl chloride (PVC) and polyethersulfone (PES) foams.

During the manufacturing of PVC foams, PVC particles are exposed to elevated temperatures to soften the polymer, and isocyanides are mixed into the PVC particles to commence both chemical cross linking and expansion (foaming). The chemical structure of solid thermoplastic linear PVC polymer is different from that in the partially cross-linked foams. To produce PES foams, solid PES polymer particles are heated close to its melting point and then carbon dioxide is injected to commence the foaming process. In this case, the foaming process should not change the chemical structure of the thermoplastic PES polymer.

The fracture behavior of polymer foams has been investigated both experimentally and analytically. Gibson and Asbhy [2] developed a fracture model for analysis of the fracture toughness, K_{IC}, of open cell foams based on bending failure of the cell edges in front of the crack tip, and assumption that the remainder of the foam can be

treated as a continuum. In closed cell foams, such as the PVC and PES foams examined here, the cell edges are connected by membranes. Maiti et al. [3] developed a model for fracture of closed cell foams and derived an expression for the fracture toughness, K_{IC}, similar to the one derived by Gibson–Ashby for open foams. The results from these models show that K_{IC} falls rapidly with decreasing density of the foam and hence that low density foams may be extremely brittle. Experimental studies of fracture of polymer foams have mostly focused on PVC foams. Zenkert and Bäcklund [4] tested PVC foams using the single edge notch beam (SENB) test and found that K_{IC} decreased with increased cell size at a constant foam density. Viana and Carlsson [5] similarly determined the mode I fracture toughness of PVC foams using SENB specimen and verified that the fracture toughness increased with increasing foam density. Shivakumar and Smith [6] examined the debond toughness (critical energy release rate) of asymmetric double cantilever beam (DCB) sandwich specimen with PVC foam core with the crack at the upper face/core interface. They found that G_{IC} was larger than G_{IC} for the pure foam measured using the SENB test [5]. The PES foam is a fairly recent foam material and has not been discussed much in the open literature.

In this work, fracture testing is conducted using two fracture test specimens, viz the SENB and DCB specimens to investigate the fracture behavior of PVC and PES foams. The SENB specimen is well known, while the DCB sandwich specimen is a symmetric sandwich DCB introduced in this study, where the crack propagates in the foam along the center of the beam.

Experimental

Materials and test specimens

The foams examined in this study are PVC and PES. Table 1 lists properties of the H (PVC) and F (PES) series foams as listed in DIAB material data sheets [7]. The

Table 2 Material properties of solid PVC and PES [2, 8, 9]

	ρ (kg/m^3)	E (GPa)	σ_{ys} (MPa)	G_{IC} (kJ/m^2)
PVC	1.40	2.7	55.0	2.02
PES	1.37	2.70	90.0	2.60

numbers next to "H" and "F" represent the nominal foam density (kg/m^3). Properties of the solid PVC and PES polymers are listed in Table 2 [2, 8, 9]. It should be reemphasized that the cellular PVC has a cross-linked chain structure whereas the solid PVC (Table 2) is not cross-linked.

Microstructural characterization

The cell structure was examined by placing small foam samples in a scanning electron microscope (FEI: Quanta 200) which includes built-in software for image analysis. The average cell size of each foam was determined using ASTM D3576 [10]. A reference line was drawn on the foam image, the number of cell intersections was recorded, and the average cell size was calculated. For determination of the cell wall thickness of each foam, 10 cell walls were measured and the results averaged. The density of each foam was measured according to ASTM D1622 [11]. Specimens of dimensions $50.8 \times 50.8 \times 25.4$ (mm) were cut. The density was obtained simply from the mass divided by the volume of the specimens.

Fracture testing

The PVC and PES foams were delivered as 12.7 and 25.4 mm thick panels from DIAB. Fracture testing of the PVC foams was conducted according to ASTM D5045 [12] utilizing the SENB configuration and a sandwich DCB specimen to be described later. The SENB specimens were cut on a standard table saw into rectangular pieces having nominal dimensions of $127L \times 25.4W \times 13.9B$ (mm) for the SENB test shown in Fig. 1. ASTM D5045 [12] specifies a specimen height, W, at least two times the thickness,

Table 1 Material properties of PVC (denoted by H) and PES foams (denoted by F) [7]

Material	Tensile modulus (MPa)	Tensile strength (MPa)	Compressive modulus (MPa)	Compressive strength (MPa)	Shear modulus (MPa)	Shear strength (MPa)
H45	55.0	1.40	50.0	0.60	15.0	0.56
H60	75.0	1.80	70.0	0.90	20.0	0.76
H100	130	3.50	135	2.00	35.0	1.60
F50	17.6*	1.60	30.0	0.40	7.50	0.60
F90	22.7*	2.15	40.0	0.70	9.50	1.10
F130	66.1*	2.70	50.0	1.00	11.5	1.60

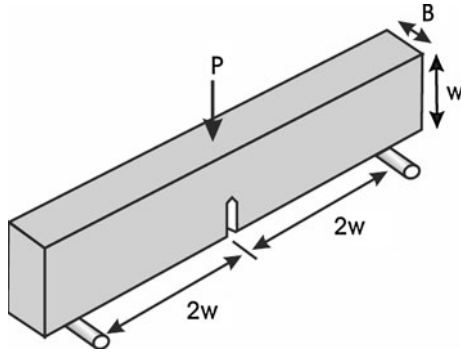* Data from Saenz et al. [19]

Fig. 1 SENB fracture specimen

Fig. 2 DCB fracture specimen

B, for a SENB specimen. However, since these specimens were cut on a table saw, it was difficult to cut the specimens any thinner than 13.9 mm. ASTM D5045 recommends that the initial crack length, *a*, should be 0.45–0.55 times the height, *W*, of the specimen. A mill with a 0.45 mm thick "circular slitting saw blade" was used to pre-notch the specimens to achieve a crack of nominal length of 6.35 mm. A fresh razor blade was tapped to sharpen and extend the pre-notched tip to a final nominal length of 13 mm. The specimen dimensions and crack length were recorded.

The SENB specimens were tested in a three-point bend fixture (with a span length, 4*W*, of 102 mm), at a crosshead rate of 12.7 mm/min while the load versus cross head displacement curves (P–δ) were recorded. An unnotched beam specimen was also tested according to ASTM D5045 to determine the specimen deformation due to the pin loading onto the foam.

Single edge notch beam (SENB) specimens were also prepared from the PES foam, in a similar manner as described above, however fracture testing revealed that the specimens failed by extensive plastic yielding prior to crack propagation which invalidated this fracture test. Zenkert et al. [13] used a compact tension specimen of very large dimensions to examine cyclic crack growth in PVC and PMI foams, but there is no reason to expect such a geometry being more successful for testing of ductile PES foams. To supplement this issue, fracture of the PES foams was examined using a new foam test in the form of a sandwich DCB specimen. Unfortunately, there is no standard for determining G_{IC} using DCB testing for a sandwich beam, although the ASTM standard for DCB testing of monolithic composites, ASTM D5528 [14], is helpful. The foam was cut into $25.4B \times 25.4T \times 200L$ (mm) and $25.4B \times 12.7T \times 200L$ (mm) blocks, where *B*, *T*, and *L* denote the width, thickness, and length of the blocks. For completeness and comparison to the SENB test results, PVC foam sandwich DCB specimens ($25.4 \times 12.7 \times 200$ (mm)) were also prepared and tested. The blocks were bonded to 6.35-mm thick aluminum plates to achieve a
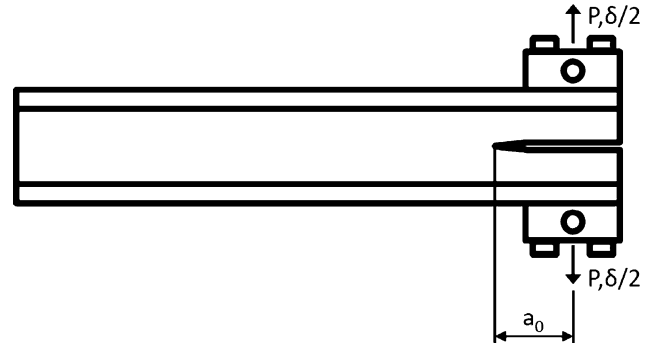
sandwich DCB test configuration as shown in Fig. 2. The aluminum adherends ensures that the specimens do not fail prematurely. Again using a 0.45-mm thick "slitting saw blade", a 45-mm pre-notch was machined at the foam midplane at the front end of each specimen. A fresh razor was then used to sharpen the initial artificial crack. The DCB specimens were loaded until the crack visually propagated about 6 mm. The loading was stopped and the new crack length recorded, and then the specimen was unloaded. The compliance, $C = \delta/P$, was determined by taking the inverse of the slope of the linear region of the load–displacement curve (P–δ). The critical load and displacement at onset of crack propagation (P_c and δ_c) were recorded based on visual observation of the crack tip region. This procedure was continued a minimum of 10 times to provide multiple G_c values for each specimen. The DCB testing was conducted in displacement control at a cross head rate of 2.54 mm/min on a Tinius-Olsen universal test machine using a 1.33-kN capacity load cell.

A minimum of three replicate SENB and DCB specimens were tested.

Data reduction for G_c

The energy release rate G_c was reduced from the fracture energy, U, recorded in the SENB test results using

$$G_c = \frac{n_e}{B(W - a)} \qquad (1)\leftarrow$$

where η_e is a crack length calibration factor tabulated in [12], U is the area the under the P–δ graph, corrected for indentation using unnotched specimens as explained in [12], *B*, *W*, and *a* are the specimen thickness, height, and initial crack length (Fig. 1). To determine the critical load for crack propagation, P_c, the ASTM 5045 [12] requires plotting of a line having 5% less slope than the initial slope onto the P–δ graph. The intersection of this line and the P–δ curve defines the critical load P_c. For a valid test P_{max}/P_c should be less than 1.1. Furthermore, according to

ASTM 5045 [12], to ensure plane strain fracture, the specimen thickness, crack length, and ligament length must exceed 2.5 times the square of the ratio K_{IC}/σ_{ys}, where K_{IC} is the critical stress intensity factor and σ_{ys} is the yield strength.

Data reduction for the DCB tests of the PES foams employs the modified beam theory (MBT) method to determine G_{IC} as outlined in ASTM D5528 [14]. According to this method the cube root of compliance, $C^{1/3}$, is plotted versus crack length, a, to generate a straight line. The x-intercept of the line provides a virtual crack length $|a| = \Delta$, which is a correction factor added to the actual crack length to enable use of ordinary beam theory. G_{IC} is determined using

$$G_{IC} = \frac{3P_c\delta_c}{2B(a + \Delta)} \leftarrow \qquad (2)\leftarrow$$

where P_c is the critical load, δ_c the critical opening displacement at the point of load application, B the specimen width, and a the crack length. This method allows construction of a fracture resistance curve (R-curve) by plotting the G_{IC} values versus crack length.

Results and discussion

Foam microstructure

The densities of the foams, Table 3, do not show any significant variability and are all relatively close to the nominal values targeted by the manufacturer. Figures 3 and 4 show typical SEM micrographs of the PVC foams (H45, H60, H100) and PES foams (F50, F90, F130). Based on such micrographs it is possible to determine the cell size and cell wall thickness. The results, summarized in Table 3, reveal that there is substantial dispersion in cell size and wall thickness as a result of the randomness of the manufacturing process. The PVC cell size decreases and the wall thickness increases slightly when the foam density is increased. For the PES foams, the cell wall thickness increases with foam density. The cells are in the range 0.4–0.9 mm for both foams. The wall thickness of the PES

Table 3 Density, cell size, and cell wall thickness of foams

Foam	Density (kg/m³)	Cell size (mm)	Cell wall thickness (μm)
H45	48.3 ± 0.39	0.84 ± 0.11	4.75 ± 2.23
H60	54.9 ± 0.63	0.67 ± 0.06	6.05 ± 2.40
H100	107 ± 1.79	0.49 ± 0.06	7.47 ± 3.10
F50	54.3 ± 0.84	0.44 ± 0.08	8.65 ± 1.26
F90	86.0 ± 4.04	0.73 ± 0.03	11.1 ± 1.65
F130	125 ± 4.53	0.76 ± 0.10	14.1 ± 4.93

foam, however, is about twice that for PVC foam of similar density.

Foam fracture response

Figure 5 shows representative load–displacement graphs from SENB tests of the H45, H60, and H100 PVC foams. All specimens failed by crack propagation in a brittle
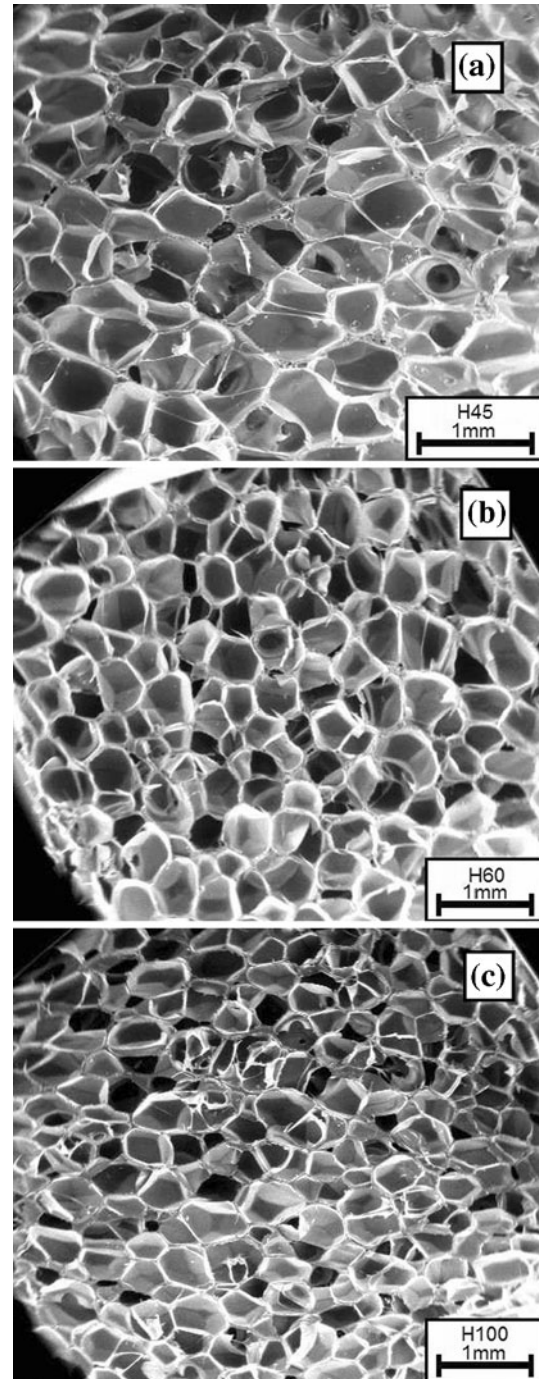

Fig. 3 SEM micrographs of PVC foams. **a** H45, **b** H60, **c** H100
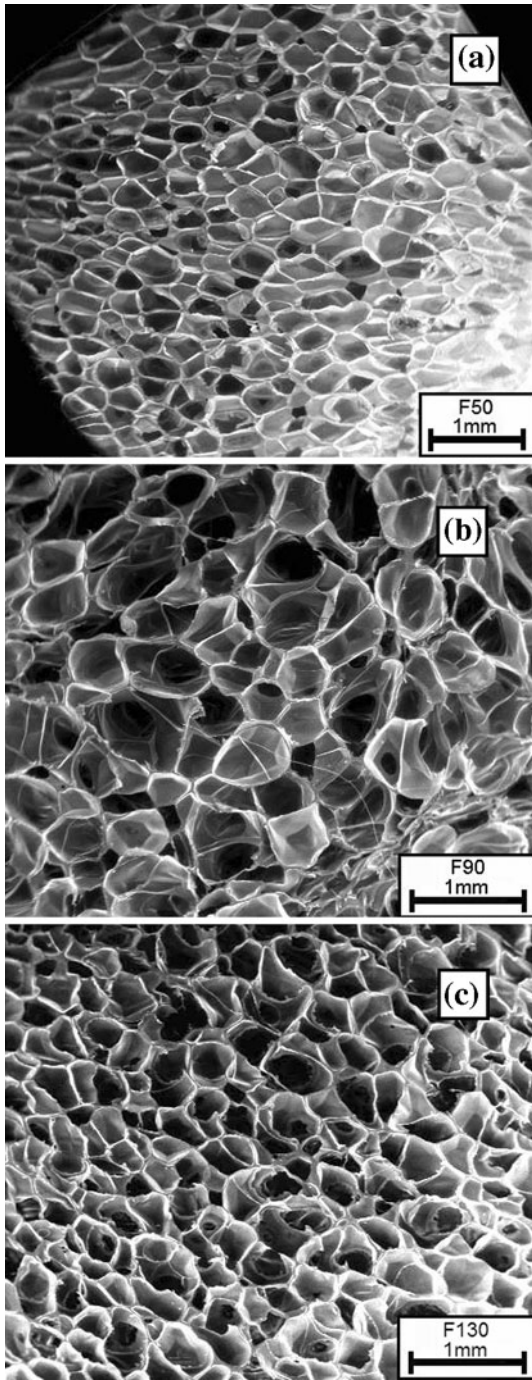
Fig. 4 SEM micrographs of PES foams. **a** F50, **b** F90, **c** F130

Fig. 5 Load–displacement curves for PVC foam SENB specimens. **a** H45, **b** H60, **c** H100

manner. This is consistent with previously reported fracture tests on PVC foams [5, 6, 15]. As mentioned earlier, SENB testing of the PES foams was unsuccessful due to the ductile nature of this foam, and for this reason the DCB specimen, Fig. 3, was used. When conducting DCB testing on a 25.4-mm thick F130 foam, however, the crack did not propagate through the center but veered off towards one of the aluminum adherends. This is likely due to the large

tensile stresses acting on planes parallel to the crack plane (*T*-stress) which promotes crack kinking and will be investigated in a separate study. To reduce the bending stress, the foam thickness was reduced by a factor of two to 12.7 mm which was found to prevent crack kinking. A 12.7 mm thickness was used also for the H45, H60, and H100 PVC DCB specimens.

Figure 6 displays typical DCB load–displacement curves for the PVC (H45, H60, H100) foams. The first curve represents crack propagation from the razor blade-sharpened crack tip. After initiation of crack growth from the razor-sharpened tip, the crack tended to propagate stably. Subsequent crack increments in the PVC foams
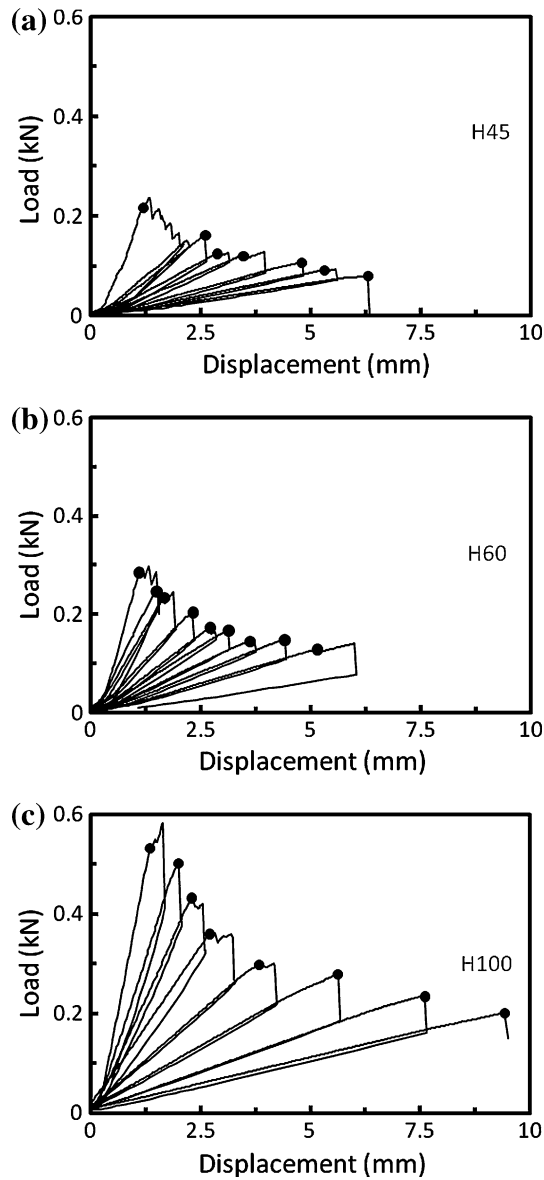
Fig. 6 Load–displacement curves for PVC foam DCB sandwich specimens **a** H45, **b** H60, **c** H100

Fig. 7 Load–displacement curves for PES foam DCB sandwich specimens **a** F50, **b** F90, **c** F130

displayed stick–slip crack growth as described by Li and Carlsson [16]. Figure 7 displays typical DCB load–displacement curves for the PES (F50, F90, F130) foams. All PES foams displayed stable crack propagation followed by non-linear load–displacement response (Fig. 7). The filled circle on each loading curve represents the point where crack propagation was visually observed used as the critical load and displacement (P_c and δ_c) in the reduction of G_{IC}, Eq. 2. Based on the measured load–displacement curves, the specimen compliance was evaluated at each crack length. Figure 8 shows an example of a plot of $C^{1/3}$ versus crack length for a PES (F50) foam. The line fitted to the $C^{1/3}$ data extrapolated to $C = 0$ provides the correction factor Δ in Eq. 2. Δ was established to be in the range from
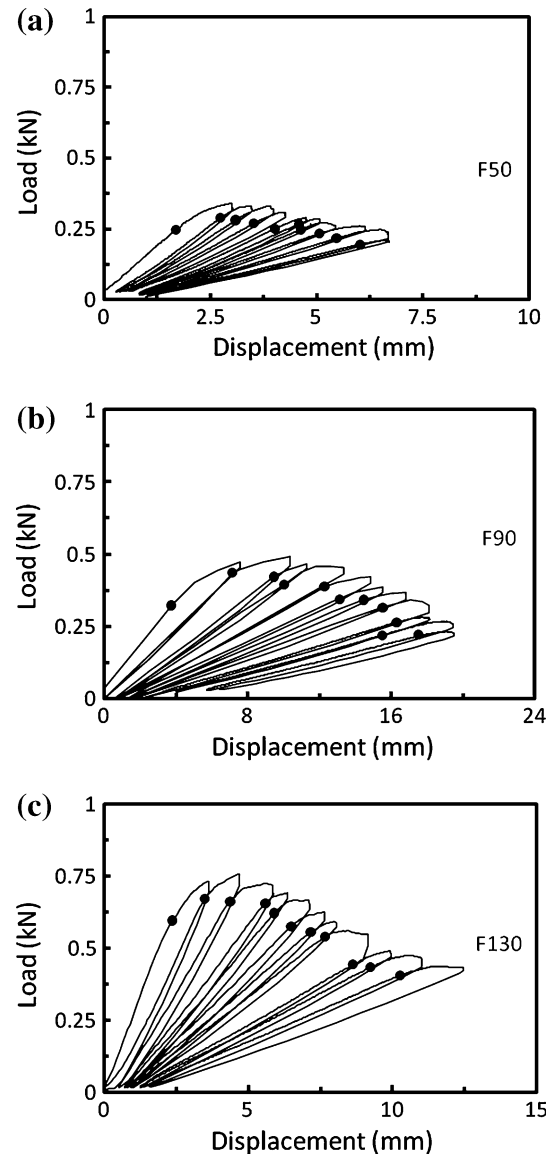
40 to 50 mm and independent of foam thickness. Each crack increment was used to determine multiple G_c values for each test specimen. This generates a fracture resistance curve (*R*-curve).

Figure 9 shows *R*-curves for the PVC foams where each symbol represents a tested specimen and where the unfilled symbol is the initial (artificial crack) critical energy release rate. The toughness of the PVC foam remains virtually constant over the range of crack lengths tested. As found by previous investigators [4–6, 15, 16], G_c increases with foam density. For the PES foams, the *R*-curves in Fig. 10 show that the initiation toughness is much less than the propagation toughness. It appears as the low initial G_c of the PES foams is due to the razor-sharpened crack tip. The crack tip in the ductile PES foams becomes blunt by the
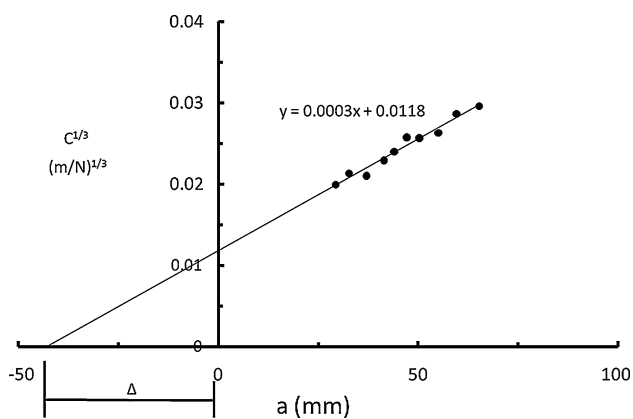
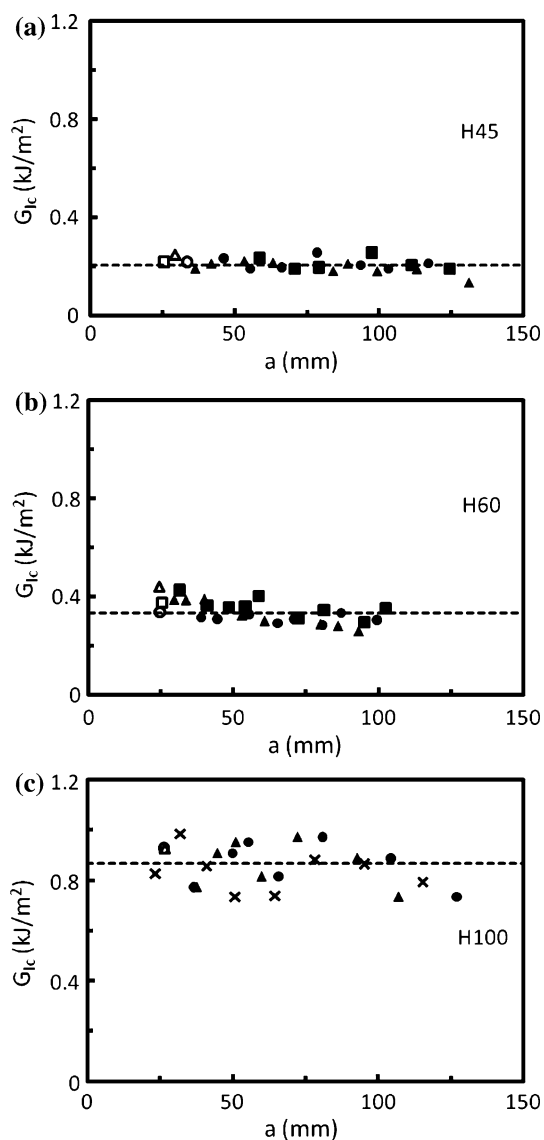Fig. 8 $C^{1/3}$ versus crack length curve for DCB test of F50 foam

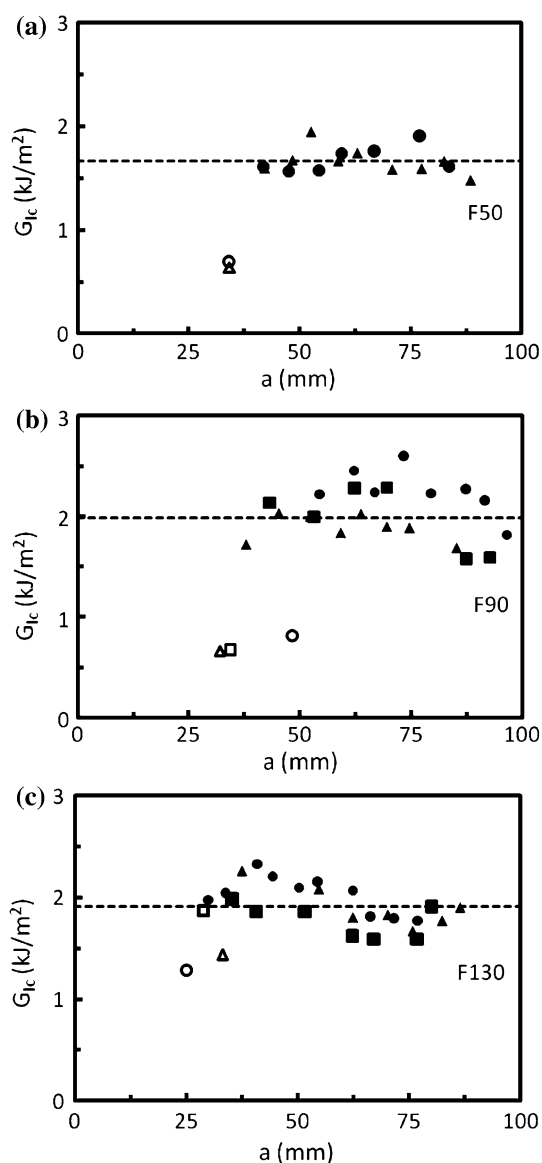Fig. 9 Fracture resistance curves for PVC foams. **a** H45, **b** H60, **c** H100

Fig. 10 Fracture resistance curves for PES foams **a** F50, **b** F90, **c** F130

local yielding of the material. The large strains at the sharp crack tip cause the crack to blunt, which would reduce the stress intensity and increase the fracture resistance. Overall, the G_c values of the PES foams displayed more scatter than the PVC foam, and much higher values.

Results from the fracture tests conducted are summarized in Table 4. The DCB test results are separated into two categories: initial (the initial razor-sharpened crack G_c) and propagation toughness. For the PVC foams, the SENB test exhibited significantly lower toughness (almost 50%) than the DCB test. Zenkert and Bäcklund [4] showed that the fracture toughness, K_{IC}, and G_c, for a H200 PVC foam decreased as the loading rate increased. Zenkert and Bäcklund [4] tested the foam over a range of crosshead

Table 4 Critical energy release rates G_{IC}(kJ/m^2) for PVC and PES foams

Material	SENB	DCB	
		Initial	Propagation
H45	0.11 ± 0.01	0.24 ± 0.03	0.20 ± 0.03
H60	0.24 ± 0.01	0.38 ± 0.04	0.33 ± 0.04
H100	0.43 ± 0.04	0.89 ± 0.05	0.87 ± 0.09
F50	–	0.58 ± 0.15	1.67 ± 0.13
F90	–	0.72 ± 0.08	1.99 ± 0.33
F130	–	1.53 ± 0.30	1.91 ± 0.21

Fig. 11 Gibson–Ashby plots for fracture toughness, G_{IC}, of PVC and PES foams. **a** PVC, **b** PES

is also likely that the foam fracture resistance is different in different planes of crack propagation; in the plane of the foam (DCB), and out-of-plane (SENB). The SENB G_c results for the PVC foams agree reasonably with those determined by Viana and Carlsson [5]. The G_c values determined for the PVC foams with the DCB test match well with the debond test results of Shivakumar et al. [17].

The critical energy release rate and density of each foam were normalized by the toughness and density of the solid host polymer (Table 2) and plotted versus relative foam density in a "Gibson–Ashby" manner. Figure 11 shows such normalized plots for the PVC and PES foams. The relatively thin cell walls of the foams should promote plane stress on a local level which elevates the toughness of ductile materials [18]. The high toughness of the PES foams is to a great part attributed to its ductile nature. Note that the toughness values of both the F90 and F130 foams approach G_c of the solid PES host polymer. The cell wall thickness of the PES foams was almost a factor of two larger for the PES foams than the PVC foams which, in addition to the ductile nature of the thermoplastic polymer, should strengthen the foam and contribute to the high toughness (G_c), see Gibson and Ashby [2].

Conclusion

The fracture behavior of a range of PVC and PES foams has been examined using SENB and DCB tests. The slightly cross-inked PVC foams failed in a linear elastic brittle manner, whereas the thermoplastic PES foams displayed much more ductility and substantially larger toughness values at a comparable foam density. It was found that the ductile PES foams displayed toughness values close to its solid counterpart whereas the toughness of the PVC foams falls substantially below its solid counterpart. The cell walls in the PES foams are almost twice as thick as in the PVC foams which, in addition to the ductile nature of the thermoplastic polymer, should contribute to the high fracture toughness. The relatively low toughness of the PVC foams is to a large extent attributed to the cross-linked nature of the polymer in the cell walls.

speeds from 1 to 10 mm/min. The reduction in G_c was in average about 10% per decade of strain rate increase. The DCB tests were run at 1.27 mm/min whereas the SENB were conducted at 12.7 mm/min as specified by the ASTM D5045 standard [12]. The higher testing speed for the SENB test may explain part of the difference, but not all. It

References

1. Zenkert D (1997) Handbook of sandwich construction. Engineering Materials Advisory Services Ltd, London, London

2. Gibson LJ, Ashby MF (1988) Cellular solids structure and properties, 1st edn. Pergamon Press, Cambridge
3. Maiti S, Ashby M, Gibson L (1984) Scripta Metall 18:213
4. Zenkert D, Bäcklund J (1989) Compos Sci Technol 34(3):225
5. Viana GM, Carlsson LA (2002) J Sandw Struct Mater 4(2):99
6. Shivakumar KN, Smith SA (2004) J Compos Mater 38(8):655
7. DIAB products-Divinycell (2004) DIAB Group. http://www.diab group.com/americas/u_products/u_prods_2.html Accessed 2009
8. Ultrason 1010 PES: Product Information (2004) BASF. http://worldaccount.basf.com/wa/EU/Catalog/ePlastics/info/BASF/product/ultrason_e_1010 Accessed 2009
9. Torlon Polyamide-imide Design Guide (2009) Solvay Advanced Polymers. http://www.solvayadvancedpolymers.com/static/wma/pdf/9/9/7/Torlon_Design_Guide.pdf. Accessed 2009
10. ASTM D3576-04 Standard test method for cell size of rigid cellular plastics
11. ASTM D1622-03 Standard test method for apparent density of rigid cellular plastics
12. ASTM D5045-99 Standard test methods for plane-strain fracture toughness and strain energy release rate of plastic materials
13. Zenkert D, Shipsha A, Burman M (2006) J Sandw Struct Mater 8(6):517
14. ASTM D5528-01 Standard test method for mode I interlaminar fracture toughness of unidirectional fiber-reinforced polymer matrix composites
15. Prasad S, Carlsson LA (1994) Eng Fract Mech 47(6):813
16. Li X, Carlsson LA (1999) J Sandw Struct Mater 1(1):60
17. Shivakumar KN, Chen H, Smith SA (2005) J Sandw Struct Mater 7(1):77
18. Anderson T (2005) Fracture mechanics: fundamentals and applications, 3rd edn. CRC Press, Boca Raton
19. Saenz E, Carlsson LA, Acha BA, Karlsson AM (2010) In: 9th international conference on sandwich structures, Pasadena